

## Roll angle estimator based on angular rate measurements for bicycles

Emilio Sanjurjo, Miguel A. Naya, Javier Cuadrado & Arend L. Schwab

To cite this article: Emilio Sanjurjo, Miguel A. Naya, Javier Cuadrado & Arend L. Schwab (2019) Roll angle estimator based on angular rate measurements for bicycles, Vehicle System Dynamics, 57:11, 1705-1719, DOI: [10.1080/00423114.2018.1551554](https://doi.org/10.1080/00423114.2018.1551554)

To link to this article: <https://doi.org/10.1080/00423114.2018.1551554>



Published online: 04 Dec 2018.



Submit your article to this journal [↗](#)



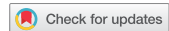
Article views: 161



View related articles [↗](#)



View Crossmark data [↗](#)



# Roll angle estimator based on angular rate measurements for bicycles

Emilio Sanjurjo <sup>a</sup>, Miguel A. Naya <sup>a</sup>, Javier Cuadrado <sup>a</sup> and Arend L. Schwab <sup>b</sup>

<sup>a</sup>Escuela Politecnica Superior, University of A Coruña, Ferrol, Spain; <sup>b</sup>BioMechanical Engineering, Delft University of Technology, Delft, Netherlands

## ABSTRACT

Measuring the roll angle of single-track vehicles has always been a challenging task; however, accurate and reliable measurements of this magnitude are paramount for controlling the stability of these vehicles, both for autonomous riding and for safety reasons. A roll angle estimation is also useful in other situations, such as tests to perform the identification of the parameters of the rider control. In this work, a new algorithm is presented for estimating the roll angle of bicycles. This estimator, based on the well-known Kalman filter, employs a wheel speed sensor to approximate the speed of the vehicle, and three angular rate sensors, which are currently small and affordable sensors. The proposed method was implemented in a microcontroller and tested in a bicycle and the results were compared with measurements obtained with optical sensors, showing a good correlation. Although it has not been tested in motorcycles, comparable results are expected.

## ARTICLE HISTORY

Received 10 July 2018  
Revised 8 November 2018  
Accepted 15 November 2018

## KEYWORDS

Roll angle estimator; bicycle; single-track vehicle; Kalman filter; inertial sensors

## 1. Introduction

Traffic accidents are one of the top 10 causes of fatalities around the world, being the first among people aged 15–29 [1]. In developed countries, the improvement of the roads and the safety features implemented in automobiles resulted in a great reduction of casualties. However, accidents concerning single-track vehicles (STV; motorcycles and bicycles) have not followed the same trend. One of the reasons is that their dynamics are highly affected by the roll (lean) angle, which has to be taken into account in any control algorithm [2]. The roll angle with respect to the road can be measured by using distance sensors. The roll angle defined in this way is related to the lateral tyre forces. However, the absolute roll angle, which is measured with respect to gravity, is directly related to the balance of any STV. Moreover, this magnitude is also useful in other kinds of situations, such as rider control parameter identification experiments. Unfortunately, there is no sensor which can measure the absolute roll angle of a STV directly, hence an estimation is needed. Several examples requiring roll angle measurements of an STV can be found in the literature, and different solutions have been applied so far. For example, in [3], a third wheel was installed

on one side of a motorbike to measure the lean angle. Similarly, in [4], a trailer was used for the roll angle measurement of a bicycle. In [5], an optical system using reflective markers was employed to measure the lean angle of a bicycle on a treadmill, and in [6], a similar setup was used for a bicycle on training rollers. In short manoeuvres, the integration of a roll rate sensor is usually enough to get the required measurement, as in [7,8]. A more complete system, which combines a high-accuracy GPS with an inertial measurement system (IMU), is used in [9] to provide the motorcycle position and attitude.

The main aim of this paper is to present and validate an absolute roll angle estimation technique for a bicycle. The method should have low computational requirements and rely on inexpensive and reliable sensors. Although we think that this method should behave properly when installed on a motorbike, the scope of this paper is limited to the application of the roll angle observer for bicycles.

There are several works in the literature dealing with state estimation of STVs. However, many of them are based on dynamical models of the vehicle and the rider. The advantage of these approaches is that they provide much more information than the lean angle. On the other hand, in order to achieve a good model, accurate force and mass distribution parameters are required. In addition, force measurements are usually required to introduce the rider action or, at least to characterise the rider control. One of these works is [10], in which a dynamical model derived from a multibody model is used in an extended Kalman filter to estimate several magnitudes of the motorcycle, including the roll angle. In [11], an unknown-input high-order sliding-mode observer is applied to the model of a motorcycle. The fuzzy logic approach has also been applied to the estimation of the states of motorcycles using dynamical models [12].

There are some other works which do not need the dynamical model of the vehicle and are based either on artificial vision or on inertial measurements. From them, the methods based on inertial measurements require less computational power and they are more suitable to be installed on a vehicle, since the hardware is less expensive and the sensors can be protected and are not affected by the possible adverse visibility conditions nor water, dust, etc. In [13,14], a roll angle observer based on the frequency separation is presented and experimentally validated. The results are good, but four expensive single-axis angular rate sensors in a special configuration are used, not allowing for the use of commercial three-axis angular rate sensors, and the method is evaluated only with roll angles up to  $25^\circ$ . Nevertheless, this roll angle observer is the best one published up to this time. In [15], two nonlinear Kalman filters (an EKF and an UKF) were compared, obtaining similar results. The setup is quite similar to that of the previous work, but only three angular rate sensors were used in this work. The results are not as accurate as in the previous work, although the method was evaluated with greater roll angles.

A comparative of four methods is presented in [16]. Two of them are based on inertial measurements, while the other two are video-based methods. The inertial methods have similarities with the ones presented in [13,15,17]. The results, however, are worse than the one presented in [13]. The errors of the video-based methods are about the same magnitude than the ones obtained with the inertial methods.

In [18], inertial measurements are combined with force measurements to estimate the pose of a bicycle and its rider. Although this paper presents interesting results, the need for force measurements makes this system expensive, since it requires installing custom-made parts on the bicycle.

A method based on acceleration measurements was used in [19] to measure the roll angle during steady-state cornering manoeuvres.

In [20], a navigation algorithm is proposed for a scooter. This algorithm needs also the lean angle, which is obtained through an artificial vision system using an on-board camera, and then it is used in the data fusion algorithm which provides the navigation output. The methods based on the artificial vision are less suitable to be implemented in commercial vehicles due to the aforementioned reason, and therefore, we will focus on a method based on inertial sensors.

In the present work, a new roll angle observer is presented and experimentally validated using an instrumented bicycle. The method employs a three-axis angular rate sensors and velocity measurements from a wheel speed sensor. The different sources of information are fused by means of a Kalman filter. The method developed in this work requires only inexpensive sensors and little computational power to be implemented, allowing to install it even in conventional and electric assisted bicycles without a significant increase of the cost nor the weight of the vehicle.

The remainder of this paper is organised as follows: Section 2 addresses the design of the observer, including a reminder of the Kalman filter equations, and the discussion of the states, the dynamical model and the sensors considered in this method. In Section 3, the experimental setup of the bicycle employed for validation is described. The experimental results are shown in Section 4. Finally, some concluding remarks are presented in Section 5.

## 2. Roll angle estimator

The attitude of a vehicle can be expressed by means of aircraft principal axes (as shown in Figure 1), using the roll ( $\phi$ ), pitch ( $\theta$ ) and yaw ( $\psi$ ) angles, which are a particular case of the

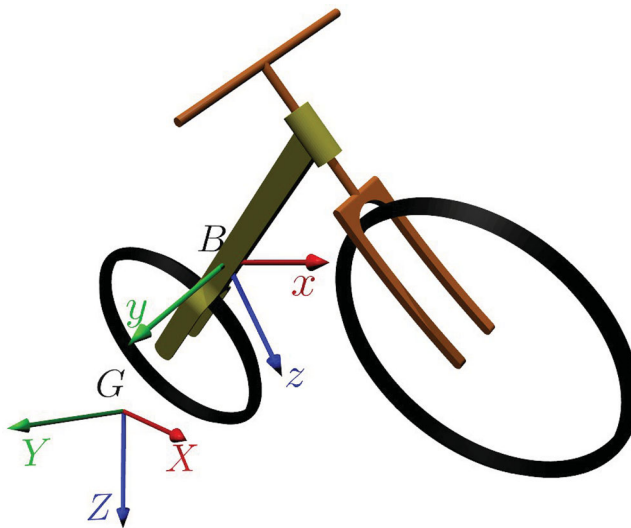


**Figure 1.** STV with axes used: a global inertial frame  $G : (X, Y, Z)$  and a body fixed frame  $B : (x, y, z)$  attached to vehicle body, here the rear frame of the STV. The orientation of  $B$  with respect to  $G$  is described the aircraft Euler angles yaw ( $\psi$ ), pitch ( $\theta$ ) and roll ( $\phi$ ).

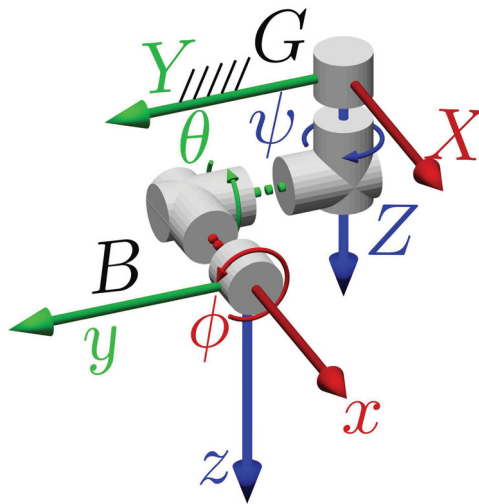


**Figure 2.** Order of yaw, pitch, roll rotations depicted by means of the ‘cans in series’ [22].

Euler angles [21]. The order of the rotations is yaw-pitch-roll if they are expressed as  $z-y-x$  intrinsic rotations or roll-pitch-yaw if they are expressed as  $x-y-z$  extrinsic rotations. The intrinsic rotations can be drawn using the so-called cans in series representation [22], as shown in Figure 2.

A vector  $\mathbf{u}^B$  expressed in the body reference system can be transformed into a vector  $\mathbf{u}^G$  expressed in the global reference system using the rotation matrix:

$$\mathbf{u}^G = \mathbf{R}_\psi \mathbf{R}_\theta \mathbf{R}_\phi \mathbf{u}^B = \mathbf{R} \mathbf{u}^B \tag{1}$$

where,

$$\mathbf{R}_\psi = \begin{bmatrix} \cos \psi & -\sin \psi & 0 \\ \sin \psi & \cos \psi & 0 \\ 0 & 0 & 1 \end{bmatrix}, \quad \mathbf{R}_\theta = \begin{bmatrix} \cos \theta & 0 & \sin \theta \\ 0 & 1 & 0 \\ -\sin \theta & 0 & \cos \theta \end{bmatrix},$$

$$\mathbf{R}_\phi = \begin{bmatrix} 1 & 0 & 0 \\ 0 & \cos \phi & -\sin \phi \\ 0 & \sin \phi & \cos \phi \end{bmatrix} \tag{2}$$

This work is focused on the estimation of the roll angle of the rear frame of an STV with respect to gravity. In order to do that, it is assumed that angular rate measurements and wheel speed sensors (WSS) are available. The angular rate sensors are assumed to be aligned with the axes in Figure 1, although if this condition cannot be met in an actual assembly, it can be solved by applying a rotation to the measurements. The selection of these sensors was conditioned by their cost and availability: WSS are already installed in every motorcycle equipped with ABS and can be easily added to bicycles (even a hub dynamo can be used if it is already installed on the bicycle), while a three-axis MEMS angular rate sensor is a very affordable and small size device, hence it is suitable to be installed in any kind of vehicle.

Several data can be extracted from the selected sensors, but they are neither accurate nor reliable measurement of the roll angle. For this reason, the different pieces of information

obtained with this set of sensors have to be combined to get the most accurate information from them. In this research, the Kalman filter was selected as the data fusion algorithm.

### 2.1. The Kalman filter

The Kalman filter is a stochastic estimator which combines predictions from a model with measurements coming from sensors. The equations of the discrete version of Kalman filter are reproduced here for the sake of clarity, where the reader interested in a detailed description of the method is referred to specific books on the topic, such as [23] or [24].

First, the state  $\mathbf{x}$  and the covariance matrix of its estimation error  $\mathbf{P}$  is predicted by means of the model:

$$\hat{\mathbf{x}}_k^- = \mathbf{F}\hat{\mathbf{x}}_{k-1}^+ + \mathbf{G}\mathbf{u}_{k-1} \quad (3a)$$

$$\mathbf{P}_k^- = \mathbf{F}\mathbf{P}_{k-1}^+\mathbf{F}^\top + \boldsymbol{\Sigma}^P \quad (3b)$$

where  $\mathbf{F}$  stands for the transition model of the system,  $\hat{\mathbf{x}}_k^-$  is the estimation of the state vector in time step  $k$  before the measurement is applied,  $\hat{\mathbf{x}}_{k-1}^+$  is the estimation of the state vector of the  $k-1$  time step after the correspondent measurements have been applied,  $\mathbf{G}$  is the input matrix,  $\mathbf{u}_k$  is the input of the system, and  $\boldsymbol{\Sigma}^P$  is the covariance matrix of the plant noise, which represents the uncertainty of the model.

After the prediction is done, the correction stage is executed:

$$\mathbf{y}_k = \mathbf{o}_k - \mathbf{H}\hat{\mathbf{x}}_k^- \quad (4a)$$

$$\mathbf{S}_k = \mathbf{H}\mathbf{P}_k^-\mathbf{H}^\top + \boldsymbol{\Sigma}^S \quad (4b)$$

$$\mathbf{K}_k = \mathbf{P}_k^-\mathbf{H}^\top\mathbf{S}_k^{-1} \quad (4c)$$

$$\hat{\mathbf{x}}_k^+ = \hat{\mathbf{x}}_k^- + \mathbf{K}_k\mathbf{y}_k \quad (4d)$$

$$\mathbf{P}_k^+ = (\mathbf{I}_g - \mathbf{K}_k\mathbf{H})\mathbf{P}_k^- \quad (4e)$$

where  $\mathbf{H}$  stands for the observation model of the system, such that  $\mathbf{y}_k$  in Equation (4a) is the mismatch (often called innovation) between the expected sensor readings according to the model ( $\mathbf{H}\hat{\mathbf{x}}_k^-$ ) and their actual values ( $\mathbf{o}_k$ ). The covariance matrix  $\mathbf{S}_k$  in Equation (4b), represents the uncertainty in the system state projected via the sensor function ( $\mathbf{H}\mathbf{P}_k^-\mathbf{H}^\top$ ) plus an additive Gaussian noise originated in the sensor itself ( $\boldsymbol{\Sigma}^S$ ). By evaluating the term  $\mathbf{K}_k$  (known as Kalman gain), the estimation of the state and its covariance are updated in Equation (4d) and Equation (4e), respectively.

### 2.2. Dynamical model of the filter

The model employed in the filter has two states: the roll angle, and the bias of the angular rate sensor along the body fixed  $x$ -axis.

The relationship among the angular rates measured by the body-mounted angular rate sensors ( $\omega_x^B, \omega_y^B, \omega_z^B$ ) and the time derivative of the roll ( $\dot{\phi}$ ), pitch ( $\dot{\theta}$ ), and yaw ( $\dot{\psi}$ ) angles of the vehicle body follows from

$$\mathbf{R}^\top \dot{\mathbf{R}} = \tilde{\boldsymbol{\omega}}^B = \begin{bmatrix} 0 & -\omega_z^B & \omega_y^B \\ \omega_z^B & 0 & -\omega_x^B \\ -\omega_y^B & \omega_x^B & 0 \end{bmatrix}, \tag{5}$$

and can be expressed as follows:

$$\dot{\phi} = \left( \omega_y^B \sin(\phi) + \omega_z^B \cos(\phi) \right) \tan(\theta) + \omega_x^B \tag{6a}$$

$$\dot{\theta} = \omega_y^B \cos(\phi) - \omega_z^B \sin(\phi) \tag{6b}$$

$$\dot{\psi} = \frac{\omega_y^B \sin(\phi) + \omega_z^B \cos(\phi)}{\cos(\theta)} \tag{6c}$$

Assuming a small pitch angle,  $|\theta| \approx 0$ , Equation (6a) becomes

$$\dot{\phi} \approx \omega_x^B \tag{7}$$

The bias ( $b_x$ ) of the  $x$  angular rate sensor ( $\omega_x^B$ ) can be modelled as a random walk, i.e. assuming that it is constant and that the variations are produced by the plant noise. Once  $b_x$  is known,  $\omega_x^B$  can be corrected. Therefore, after applying the forward Euler integration method, the dynamic model of the filter in Equation (3a) becomes:

$$\begin{bmatrix} \hat{\phi} \\ \hat{b}_x \end{bmatrix}_k^- = \begin{bmatrix} 1 & -dt \\ 0 & 1 \end{bmatrix} \begin{bmatrix} \hat{\phi} \\ \hat{b}_x \end{bmatrix}_{k-1}^+ + \begin{bmatrix} dt \\ 0 \end{bmatrix} \omega_{x,k-1}^B \tag{8}$$

where the states at the present time step  $k$  are expressed in function of the states and the inputs of the previous time step  $k-1$ , being  $dt$  the integration time step.

### 2.3. Absolute ‘measurements’ of the roll angle

In the correction stage of the Kalman filter (in particular, in Equation (4a)), absolute measurements of the roll angle are needed. However, as actual measurements of the roll angle are not usually available, they are created by using data from a wheel speed sensor and a three-axis angular rate sensor. In this work, two different approaches are employed to obtain the absolute roll angle measurements, and then both are combined into a single measurement.

The first roll angle measurement has been used by many others (e.g. [13,16,17]). It assumes a steady-state cornering motion and uses the lateral dynamics equilibrium to calculate the first estimation of the roll angle,  $\phi_d$  (see Figure 3)

$$\phi_d = \arctan\left(\frac{\dot{\psi}^2 R}{g}\right) = \arctan\left(\frac{\dot{\psi} v}{g}\right), \tag{9}$$

where  $v$  is the forward speed of the vehicle and  $R$  is the radius of the trajectory. Notice that this equation is only valid for stationary turns on level grounds. Although the two

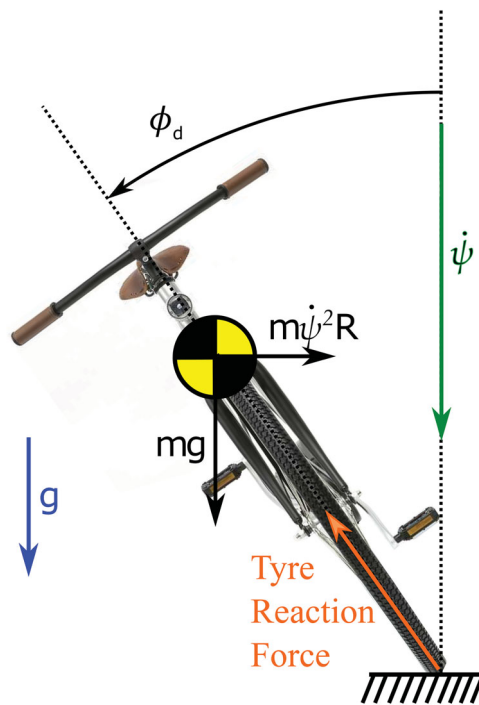


**Figure 3.** Dynamic force equilibrium during steady-state cornering.

expressions in Equation (9) are equivalent, the last one is more convenient for the implementation, since the radius of the trajectory is not involved in the equation. The speed of the vehicle is usually calculated from the angular rate of the wheels. Although this method does not provide exact velocity information, the velocity estimation is usually good enough for this application. The calculation of the yaw rate  $\dot{\psi}$  is trickier, since its exact value is related to the body angular rates through Equation (6c), which involves the roll and pitch angles. However, in this work  $\omega_z^B$  is used as an estimation of the yaw rate  $\dot{\psi}$ .

The main drawbacks of this approach are the following:

- The equations were developed with a level road in mind, so the bigger the slope, the larger error is expected.
- The cross-section of the tyres is not considered. However, if thick tyres are employed (for example, in sport motorcycles), they are going to produce some effects when the vehicle is leaned, namely:
  - The contact point of the wheels is not in the symmetry plane of the vehicle
  - The effective radius of the wheel decreases, thus the calculation of the speed of the vehicle is wrong.
- The gyroscopic effect of the wheels has an upright effect which has to be compensated by leaning more the vehicle.
- The roll angle is not properly estimated during transients (i.e., when  $\dot{\phi} \neq 0$ ), even when using high pressure, thin tyres while riding on a flat floor.
- An exact measurement of the yaw rate is not available if the roll or pitch of the vehicle are non-zero.

- This technique considers that the center of mass of the vehicle is in the symmetry plane, but it is no longer true if the rider leans or displaces laterally his body.

All these effects become more important for big roll angles, but are almost negligible when riding straight.

For big roll angles, a new approach for measuring the roll angle was developed in this work. The method is based on the existent relationship between the angular rates measured by the angular rate sensor if a null pitch rate  $\dot{\theta}$  is considered. This approximation relies on the fact that the long term mean of the pitch rate is null during riding. Introducing the null pitch rate assumption, Equation (6b) becomes:

$$0 = \omega_y^B \cos(\phi) - \omega_z^B \sin(\phi) \quad (10)$$

and the roll angle estimation  $\phi_\omega$  can be calculated as

$$\phi_\omega = \arctan\left(\frac{\omega_y^B}{\omega_z^B}\right) = \text{sgn}(\omega_z^B) \arcsin\left(\frac{\omega_y^B}{\sqrt{(\omega_y^B)^2 + (\omega_z^B)^2}}\right) \quad (11)$$

where  $\text{sgn}(\omega_z^B)$  is the sign of the z angular rate. Both versions of this equation are mathematically equivalent, but the second one is more convenient in practice, when noisy measurements taken from real sensors are used, thus avoiding the division by zero.

This approach has some advantages:

- It works well in roads with any slope, as long as the pitch rate of the vehicle is small.
- it is not affected by the tyre thickness
- It is not affected by the rider's movements
- It is not affected by the gyroscopic effect of the wheels

And also some drawbacks:

- It does not work if the vehicle is not turning
- It is usually noisier than the method based on the lateral dynamics of the steady-state cornering, specially for small roll angles.

In order to take advantage of both methods for measuring the roll angle, they are combined using a weighted mean. The weighing function changes its value depending on the last available estimation of the roll angle  $\hat{\phi}$ , taken from the state observer:

$$W = \exp\left(-\frac{\hat{\phi}^2}{\bar{\phi}^2}\right) \quad (12)$$

where  $\bar{\phi}^2$  is a constant value which can be used to adjust the behavior of the weighting function. A value of  $\bar{\phi}^2 = 0.05$  was employed in this work, with the estimated roll angle  $\hat{\phi}$  expressed in radians. This weighting function is represented in Figure 4.

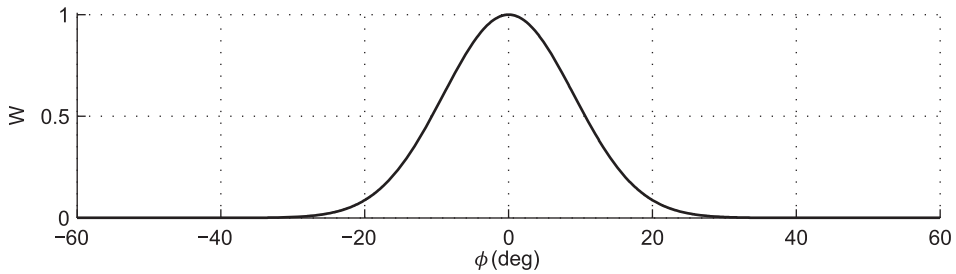


**Figure 4.** Weight function with respect to the roll angle.

The roll angle measurement  $\mathbf{o}_k$  to be employed in Equation (4a) is  $\phi_m$ , built as weighed combination of  $\phi_d$  and  $\phi_\omega$ :

$$\phi_m = W\phi_d + (1 - W)\phi_\omega \quad (13)$$

With the value of  $\bar{\phi}^2$  used here, the roll angle measurement based on the steady-state lateral dynamics is predominant when the absolute value of the roll angle is under 0.186 rad (10.67°). When the absolute value of the roll angle exceeds 0.339 rad (19.44°), more than the 90% of the weight of the roll angle measurement comes from the relationship between  $\omega_y^B$  and  $\omega_z^B$  with the null pitch rate assumption. The results from the various roll angle estimations during a manoeuvre can be seen in Figure 5. It can be appreciated that the method based on the relationship between angular velocities does not work when the vehicle goes straight, but it improves when the vehicle is leaned. The method based on the lateral dynamics of the steady-state cornering works well riding straight, but it performs bad at

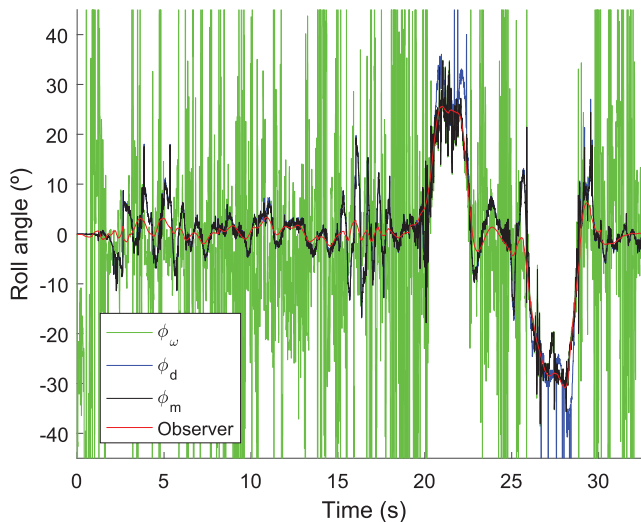


**Figure 5.** Comparison among the different roll angle estimations. The first line is roll angle estimation calculated from the relationship between  $\omega_y^B$  and  $\omega_z^B$ ,  $\phi_\omega$ . The second line is the roll angle estimation calculated from the steady-state cornering dynamics,  $\phi_d$ . The third line is the combination of both measurements  $\phi_m$  as in Equation (13). Finally, the fourth line is the estimation of the roll angle provided by the state observer.

high roll angles, or during transients. However, combining both estimations according to Equation (13) provides an improved approximation of the roll angle.

### 3. Experimental setup

In order to check the behaviour of the method in a real vehicle, a bicycle was instrumented, see Figure 6. The core of the system is an Arduino Due, a development board based on the Atmel SAM3X8E microcontroller. The Arduino acquires the data from the sensors, runs the roll angle observer, and logs the data to a SD card.

In order to run the roll angle observer, the forward speed of the bicycle and the three angular rates of the rear frame are needed. The forward speed of the bicycle was measured with a toothed crown fixed on the rear wheel and a through-beam infrared sensor (Omron EE-SX1041). The angular rates of the rear frame were measured with a three-axis angular rate sensor (STmicro L3GD20H) attached to the Arduino board.

For validation purposes, two infrared distance sensors (Sharp GP2Y0A02YK0F) were installed at both sides of the bicycle. The roll angle can be calculated from the measurements provided by these sensors using the following equation:

$$\phi = \arctan \left( \frac{D_L - D_R}{D_H} \right) \quad (14)$$

where  $D_L$  and  $D_R$  are the distances measured by the sensors on the left and on the right respectively, and  $D_H$  is the distance between the sensors measured perpendicularly to the symmetry plane of the bicycle.

However, it was found that the distance measurements are quite noisy, and they are affected by the irregularities of the road: white lines, the different height of the pavement with respect to the road, etc. For this reason, the angle is calculated using a different algorithm:



**Figure 6.** Instrumented bicycle, equipped with a photoelectric sensor to measure real wheel speed, and a three-axis angular rate sensor to estimate the roll angle. There are also two distance sensors for validation purposes.

- First, the roll angle is calculated according to the sensors of both sides, as follows:

$$\phi_L = \arctan\left(\frac{D_L - H_S}{\frac{D_H}{2}}\right) \quad (15a)$$

$$\phi_R = \arctan\left(\frac{H_S - D_R}{\frac{D_H}{2}}\right) \quad (15b)$$

where  $H_S$  is the sensor height at zero roll angle.

- Then, if both calculations of the roll angle are nearly similar ( $|\phi_L - \phi_R| < 0.3\text{rad}$ ), they are averaged. Otherwise, the one which has the larger difference with the previous roll angle calculation is discarded.
- Finally, a low pass filtering algorithm with a cutoff frequency of 2 Hz is applied.

After this process is done, the roll angle measurements from the optical sensors are quite consistent.

#### 4. Results and discussion

In order to be able to validate the roll angle observer, the tests must be performed in a flat level ground, because the optical validation system measures the roll angle relative to the ground, whereas the roll angle observer measures the roll angle with respect to gravity.

Covariance matrices of plant and measurement noise for the Kalman filter have been manually tuned from the results of some tests, resulting the following values for the plant and measurement noises,  $\Sigma^P$  and  $\Sigma^S$ , respectively:

$$\Sigma^P = \begin{bmatrix} 5e^{-7} & 0 \\ 0 & 1e^{-8} \end{bmatrix} \quad (16)$$

$$\Sigma^S = 0.1 \quad (17)$$

The values of the covariance of the plant noise are much lower than that of the measurement noise, thus emphasising the prediction of the plant model over the approximated roll angle measurements in the short term. However, the values of these parameters must be specifically tuned to be employed with other vehicle and/or other set of sensors.

All the manoeuvres started and finished with null velocity. In this situation, the rider steps on the floor to stabilise the bicycle, and the dynamics of an STV cannot be applied. For this reason, a settling time can be seen in all the tests at the beginning of the manoeuvres, and also a drift at their ending.

The first test started with a straight section. After that, a constant radius turn was performed, and finally, the bicycle was ridden straight again. Results of this manoeuvre can be seen in Figure 7. There are two big errors around 30 s, but looking at the plot, it becomes clear that those errors were produced in the optical sensors, since the manoeuvre was a constant turn, and the signal with sudden variations is the one coming from the distance sensors. This manoeuvre demonstrates that the algorithm is stable in both straight and turning conditions, and that it also works well in the transitions between both situations. The RMSE for this manoeuvre was  $1.5^\circ$ .

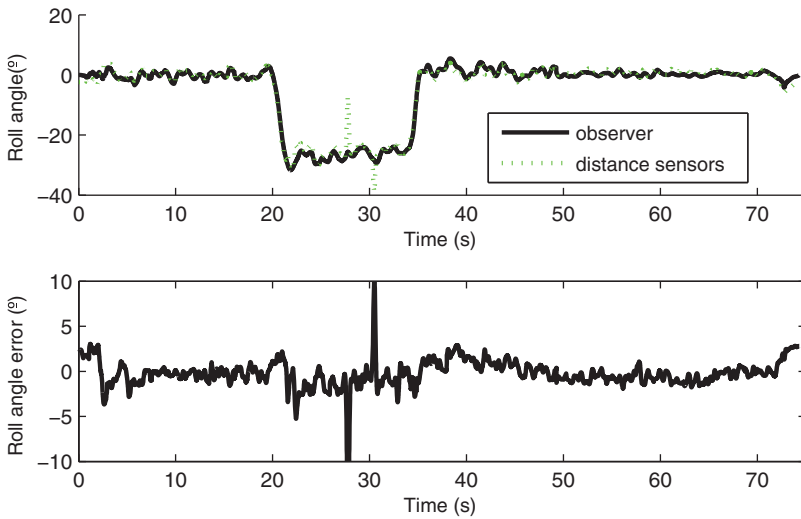


**Figure 7.** Roll angle from distance sensor (validation) and state observer during straight line/constant radius/straight line manoeuvre (counter-clockwise turn).

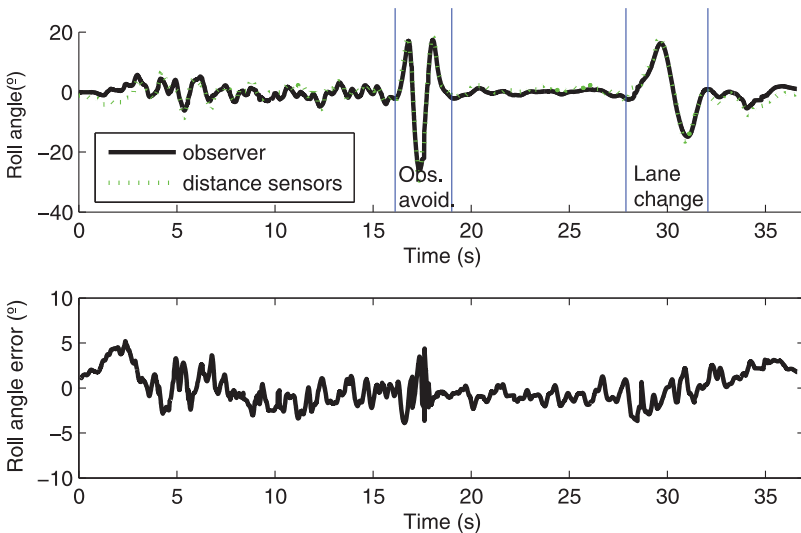


**Figure 8.** Roll angle from distance sensor (validation) and state observer during obstacle avoidance manoeuvre and lane change.

The second test conducted was a combination of obstacle avoidance and lane change (see Figure 8). The manoeuvre started riding straight. After that, three consecutive turns were performed to avoid an obstacle and return to the original trajectory. Finally, a lane change was performed. This test shows that the roll angle observer performs well in fast series of alternative turns. The RMSE for this manoeuvre was  $1.7^\circ$ .

The third test was a manoeuvre looking for the maximum roll angle, such that the bicycle was ridden at maximum speed in a sharp corner. The results are shown in Figure 9. The RMSE for this test was  $1.8^\circ$ .

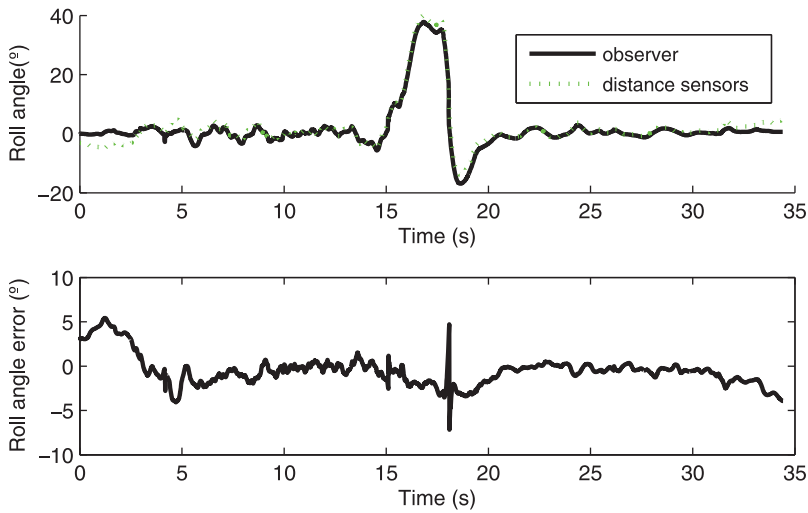


**Figure 9.** Roll angle from distance sensor (validation) and state observer during high roll manoeuvre.

The last test was executed doing normal cycling in public roads, including potholes, slopes, bank angle, etc. Since the roads are usually not flat, the measurements from the distance sensors do not provide the correct roll angle. However, this test is useful to verify the stability of the observer during normal riding conditions. The results can be seen in Figure 10. In the roll angle plot, it can be seen that the roll angle provided by the observer is always around zero, while the plot of the roll angle provided by the distance sensors has several sections in which the angle is not around zero, due to the non-zero bank angles in the several sections of the road employed for this test.

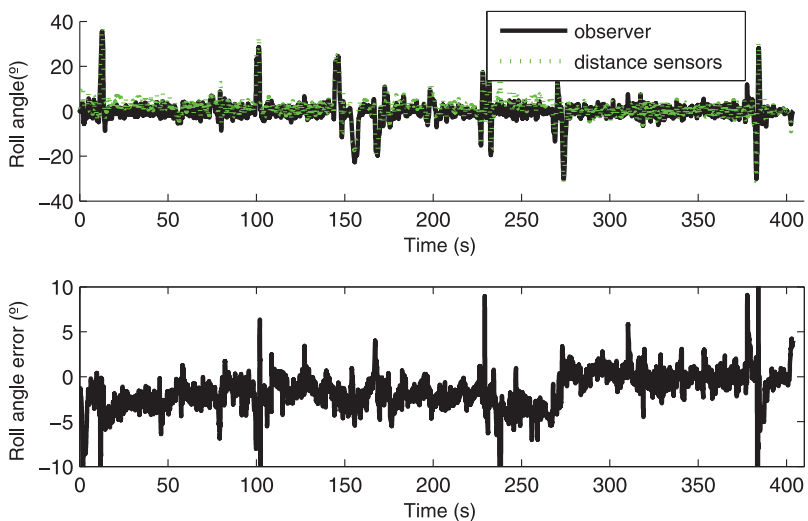


**Figure 10.** Roll angle from distance sensor and state observer during normal riding conditions.

## 5. Conclusions

This paper presents a new method for estimating the roll angle for an STV. The sensors employed for the observer are a low cost three-axis angular rate sensor and a wheel speed sensor (already available in any vehicle equipped with ABS). The roll observer employs a Kalman filter to combine information from a dynamical model of the roll angle with noisy measurements of the absolute roll angle, obtained both from the lateral dynamics of the steady-state turning, and from a kinematic relationship between the angular rates provided by the zero pitch rate assumption.

A bicycle was equipped with these sensors, a microcontroller and two distance sensors for validation purposes. Some manoeuvres were performed to check the accuracy of the method under several conditions: high roll angle, straight line to turn transition, obstacle avoidance manoeuvres and long-term performance of the algorithm. The results obtained here are among the best found in literature (RMSE < 2°), but at a considerable lower hardware cost.

## Disclosure statement

No potential conflict of interest was reported by the authors.

## Funding

This work has been partially financed by the Ministerio de Economía y Competitividad and European Regional Development Fund funds under the project 'Observadores de estados y entradas basados en modelos multicuerpo detallados aplicados al control de vehículos' [TRA2014-59435-P], by the Xunta de Galicia [ED431B 2016/031], and by the European Commission under the MOTORIST (Motorcycle Rider Integrated Safety) project (ITN Nr. 608092), funded through the FP7 Marie Curie programme. The research of Emilio Sanjurjo was funded by the Spanish Ministry of Economy and Competitiveness under the fellowship BES-2013-063598 and the grant number EEBB-I-15-10331.

## ORCID

Emilio Sanjurjo  <https://orcid.org/0000-0002-3024-911X>

Miguel A. Naya  <https://orcid.org/0000-0001-7901-8278>

Javier Cuadrado  <https://orcid.org/0000-0001-8604-6816>

Arend L. Schwab  <https://orcid.org/0000-0001-5897-9790>

## References

- [1] WHO. Global Status Report on Road Safety 2015. 2015. Available from: [http://www.who.int/violence\\_injury\\_prevention/road\\_safety\\_status/2015/en/](http://www.who.int/violence_injury_prevention/road_safety_status/2015/en/)
- [2] Corno M, Panzani G, Savaresi SM. Single-Track Vehicle Dynamics Control: State of the Art and Perspective. *IEEE ASME Trans Mechatron.* 2015;20(4):1521–1532. Available from: <http://ieeexplore.ieee.org/lpdocs/epic03/wrapper.htm?arnumber=7021936>
- [3] FU H. Fundamental Characteristics of Single-Track Vehicles in Steady Turning. *Bull JSME.* 1966;9(34):284–293.
- [4] Moore JK. Human control of a bicycle [dissertation]. Davis: University of California at Davis; 2012.
- [5] Fonda B, Sarabon N, Li FX. Bicycle rider control skills: Expertise and assessment. *J Sports Sci.* 2017 Jul;35(14):1383–1391.

- [6] Cain SM, Ashton-Miller JA, Perkins NC. On the skill of balancing while riding a bicycle. *PLoS ONE*. 2016;11(2):1–18.
- [7] Cossalter V, Sadauckas J. Elaboration and quantitative assessment of manoeuvrability for motorcycle lane change. *Vehicle Syst Dynam*. 2006 Dec;44(12):903–920.
- [8] Biral F, Bortoluzzi D, Cossalter V, et al. Experimental Study of Motorcycle Transfer Functions for Evaluating Handling. *Vehicle Syst Dynam*. 2003 Jan;39(1):1–25.
- [9] Fujii S, Shiozawa S, Shinagawa A, et al. Steering characteristics of motorcycles. *Vehicle Syst Dynam*. 2012 Aug;50(8):1277–1295.
- [10] Teerhuis AP, Jansen ST. Motorcycle state estimation for lateral dynamics. *Vehicle Syst Dynam*. 2012;50(8):1261–1276.
- [11] Nehaoua L, Ichalal D, Arioui H, et al. An Unknown-Input HOSM Approach to Estimate Lean and Steering Motorcycle Dynamics. *IEEE Trans Veh Technol*. 2014;63(7):3116–3127.
- [12] Dabladji MEH, Ichalal D, Arioui H, et al. Unknown-input observer design for motorcycle lateral dynamics: TS approach. *Control Eng Pract*. 2016;54:12–26.
- [13] Boniolo I, Tanelli M, Savaresi SM. Roll angle estimation in two-wheeled vehicles. In: 2008 IEEE International Conference on Control Applications. San Antonio, TX: IEEE; 2008. p. 31–36.
- [14] Boniolo I, Tanelli M, Savaresi S. Roll angle estimation in two-wheeled vehicles. *IET Control Theory Appl*. 2009;3(1):20–32.
- [15] Corbetta S, Boniolo I, Savaresi SM. Attitude estimation of a motorcycle via Unscented Kalman Filter. In: 5th IFAC Symposium on Mechatronic Systems. Cambridge, MA; 2010. p. 511–516.
- [16] Schlipfing M, Salmen J, Lattke B. Roll angle estimation for motorcycles: Comparing video and inertial sensor approaches. In: 2012 IEEE Intelligent Vehicles Symposium. Alcalá de Henares: IEEE; 2012. p. 500–505.
- [17] Lot R, Cossalter V, Massaro M. Real-Time Roll Angle Estimation for Two-Wheeled Vehicles. In: Proceedings of the ASME 2012 11th Biennial Conference on Engineering Systems Design and Analysis ESDA2012. Nantes: ASME; 2012. p. 687–693.
- [18] Zhang Y, Chen K, Yi J. Rider Trunk and Bicycle Pose Estimation With Fusion of Force/Inertial Sensors. *IEEE Trans Biomed Eng*. 2013 Sep;60(9):2541–2551.
- [19] Cain SM, Perkins NC. Comparison of experimental data to a model for bicycle steady-state turning. *Vehicle Syst Dynam*. 2012 Aug;50(8):1341–1364.
- [20] Guarnieri A, Pirotti F, Vettore A. Low-cost MEMS sensors and vision system for motion and position estimation of a scooter. *Sensors*. 2013;13:1510–1522.
- [21] Goldstein H. *Classical Mechanics*. Reading, MA: Addison Wesley; 1950.
- [22] Schwab AL, Meijaard JP. How to Draw Euler Angles and Utilize Euler Parameters. In: Volume 2: 30th Annual Mechanisms and Robotics Conference, Parts A and B. Philadelphia, PA: ASME; 2006. p. 259–265.
- [23] Simon D. *Optimal State Estimation: Kalman, H Infinity, and Nonlinear Approaches*. Hoboken, NJ: Wiley; 2006.
- [24] Grewal M, Andrews A. *Kalman filtering: Theory and practice using MATLAB®*. Hoboken, NJ: Wiley; 2008.